ASME Letters in Dynamic Systems and Control
Online journal at:
https://asmedigitalcollection.asme.org/lettersdynsys

Pillip M. Rivera-Ortiz
The Johns Hopkins University Applied Physics Laboratory,
11100 Johns Hopkins Road,
Laurel, MD 20723
e-mail: phillip.rivera@jhuapl.edu

Andrew C. Frommer[2]
Department of Mechanical Engineering,
Collaborative Controls and Robotics Laboratory,
University of Maryland,
College Park, MD 20742
e-mail: afromm88@umd.edu

Yancy Diaz-Mercado
Department of Mechanical Engineering,
Collaborative Controls and Robotics Laboratory,
University of Maryland,
College Park, MD 20742
e-mail: yancy@umd.edu

Contraction Analysis of Multi-Agent Control for Guaranteed Capture of a Faster Evader[1]

This work presents a verifiable condition for the selection of a sufficient number of pursuers to capture a faster evader. The condition is based on the tracking performance of a multi-agent control scheme. Trajectory tracking results are provided for both the effects of the multi-agent control topology and its execution by the pursuers in the context of input saturation. To that end, nonlinear contraction theory is leveraged because it provides a unifying framework for the analysis of systems subject to bounded disturbances. Monte Carlo simulations are performed to validate the proposed condition for sufficient pursuers selection.
[DOI: 10.1115/1.4065029]

Keywords: networked systems, robotics, pursuit-evasion games, nonlinear controls, cooperative control, networked control systems, nonlinear systems

This work analyzes the performance of multi-agent control methods in devising pursuer cooperation strategies for pursuit-evasion games. The focus is on the ε−capture problem, where a team of N pursuers tries to get ε close to a faster evader. The objective is to showcase how it is indeed possible to trade off kinematic capabilities of the pursuer agents with number of pursuers through the use of multi-agent control methods.

The motivation for selecting multi-agent control methods is threefold. First, multi-agent control is scalable to *any number* of pursuers and extendable to decentralized formulations. Second, it allows the many tools of nonlinear system analysis to completely characterize performance as a function of the number of pursuers and problem requirements, e.g., initial conditions and maximum speed. Third reason is its ease of implementation.

This work is intended to provide a complementary perspective to state-of-the-art differential game theory (DGT) approaches for pursuer cooperation explored by Refs. [1,2]. The main benefit of DGT approaches is the ability to predict a saddle point solution to the game. This means unilateral deviations from this solution only benefit the adversary. The drawback is that the synthesis of controllers for optimal formulations is notoriously hard to obtain in a closed form when considering a faster evader. Thus, results usually apply to specific instances of an engagement. An example is how optimal cooperative pursuer strategies for achieving ε-capture rely on the pursuers first achieving an encirclement configuration, which might prove unmanageable in practice.

The concept of pursuer capture through multi-agent control methods was introduced by Refs. [3,4]. The focus is on reachability and specifically on directly controlling the capture sets (also called region of dominance) of the pursuers. These sets constitute all the positions that the pursuer can reach before or at the same time as the evader. The main contribution of that work (Theorem 1 of [4]) states that a sufficient condition for capture is that the union of the pursuer's capture sets persistently separates the evader from its goal. Coordinated pursuer strategies were devised through the minimization of a surrogate control objective that aimed at ensuring the pursuer's capture set spanned a given space while remaining at least tangent.

The advantage of this formulation lies in its scalability as shown by Ref. [5], robustness explored as shown by Ref. [3], convergence properties as shown by Ref. [4], and extension from static to time-varying domains demonstrated as shown by Ref. [6]. A decentralized approach for ensuring capture-set connectivity through the use of control barrier functions was introduced by Ref. [7], which led to a decrease in the required number of pursuers. However, an explicit relationship to provide capture guarantees as a function of the number of pursuers and initial conditions is still missing.

Static conditions to provide capture guarantees as a function of the number of pursuers were proposed by Ref. [8]. The approach consisted of determining the minimum number of pursuers needed for their capture sets to completely span a worst-case coverage domain. The approach, however, did not consider the dynamic effects of tracking performance by the individual pursuers subject to maximum speed constraints. Thus, the focus of this work is to provide capture guarantees as a function of the number of pursuers by combining both the static and dynamic requirements.

The main contributions of this work are twofold: (1) an analytical framework for proving the boundedness of tracking performance for different multi-agent control topologies realized by pursuers subject to maximum speed saturation through the use of contraction theory developed by Ref. [9], as well as (2) a verifiable condition for

[1]Paper presented at the 2023 Modeling, Estimation, and Control Conference (MECC 2023), Lake Tahoe, NV, Oct. 2–5, Paper No. MECC2023-167.
[2]Corresponding author.
Manuscript received July 25, 2023; final manuscript received February 5, 2024; published online April 3, 2024. Assoc. Editor: Peter H. Meckl.

estimating the minimum number of pursuers required for guaranteed capture. This last contribution will enable the use of task allocation algorithms via formal specifications in pursuit-evasion games given their explicit requirement on task completion guarantees.

This work is organized as follows. Section 1 provides the mathematical background on contraction theory and introduction to reach-avoid (RA) games. The multi-agent control descriptions and tracking problems of interest are provided in Secs. 2 and 3, respectively. Section 4 presents the main results from this work, and Sec. 5 presents simulation verification. Section 6 presents conclusions.

The following notation is adopted throughout this work. Small letters denote vectors (x); capital letters denote matrices (X); and script font $\mathcal{X}$ denotes sets. $1_N \in \mathbb{R}^N$ is the vector of all 1s. The superscript (e) denotes the evader; (i) denotes the ith member of the pursuer team; and (p) denotes all pursuers.

1 Mathematical Preliminaries

This work leverages properties of nonlinear contracting systems to provide tracking performance bounds of multi-pursuer teams subject to saturation. Given that tracking performance will induce an error in the desired pursuer capture set, the objective of this work is to characterize the required number of pursuers such that capture guarantees can still be provided. To that end, this section provides the relevant background in contraction theory and characterization of pursuers' capture sets for fast evader games.

1.1 Contraction Theory Preliminaries. Contraction theory provides a new interpretation of system stability, which characterizes system trajectories that tend to each other, rather than convergence to a fixed state. Thus, it is said that a system is contracting if it tends to *forget initial conditions*. The reason for leveraging contraction theory results is that they can be used to provide uniform bounds in nondifferentiable norms, which are required for analyzing the worst-case performance of multi-agent systems in ensemble form. The following contraction theory results are provided for the identity metric $\Theta(x, t) = I$.

THEOREM 1. *Contraction of Ref. [9].*
A system

$$\dot{x} = f(x, t)$$

is said to be contracting if $\exists \lambda > 0$ *such that the induced p matrix measure of the Jacobian* $\mu_p\left(\frac{\partial f(x,t)}{\partial x}\right) \leq -\lambda, \ \forall x, \forall t$. *The value* λ *is denoted the contraction rate.*

For contracting nonlinear systems, this main result can be extended to provide robustness properties of a nominal system subject to bounded disturbances.

THEOREM 2. *Robustness of Ref. [10].*
Consider a nominal system $\dot{x} = f(x, t)$ *and a disturbed system* $\dot{x}_d = f(x_d, t) + g(x_d, t)$. *If the nominal system is contracting, with contraction rate* λ *in a p-norm, then the disturbed system trajectories are bounded by*

$$\|x(t) - x_d(t)\|_p \leq \|x(0) - x_d(0)\|_p \, e^{-\lambda t} + \frac{d}{\lambda},$$

where $\|g(x, t)\|_p \leq d$ *uniformly in time.*

Table 1 summarizes the matrix norm and induced matrix measure used throughout this work. In the table, q_{ij} is the ijth entry in A, and $\lambda_i(A)$ is the ith eigenvalue of A.

1.2 Differential Game Theory Preliminaries. This work considers the coordination of N pursuers against a fast evader in RA games. The evader tries to reach a goal set $\mathcal{P}$ while actively avoiding capture by the pursuer team. It is assumed that the players have bounded particle dynamics

$$\dot{x}^i = u^i, \quad \dot{x}^e = u^e \tag{1}$$

for states $x^i, x^e \in \mathbb{R}^2$, and inputs $u^i \in \{\mathbb{R}^2 | \|u^i\|_\infty \leq \bar{u}^p\}$, $u^e \in \{\mathbb{R}^2 | \|u^e\|_\infty \leq \bar{u}^e\}$. The concatenation of all pursuer states x^i is given by $x^p \in \mathbb{R}^{2N}$. Throughout this work, it is assumed that $\sigma = \bar{u}^p / \bar{u}^e < 1$, and $\sigma > 0$. The considered RA game is as follows.

PROBLEM 1. *(RA Game in Finite Time) Game of a kind in which the evader only wins if it reaches a desired target set* $\mathcal{P}$ *before a final time* t_f, *while avoiding* ε*-capture.* ε*-Capture is defined as* $\min_{i,N} \|x^i(t) - x^e(t)\| \leq \varepsilon$ *for* $t \in [t_0, t_f]$ *given a fixed* $\varepsilon > 0$.

In differential games, the capture set denotes the set of positions where the pursuer can reach the evader. The majority of the DGT work relies on simple representations of these sets using Apollonius circles as used by Ref. [11]. However, this representation becomes too conservative when considering pursuers with a finite capture radius against a faster evader. In this case, Cartesian ovals provide a better representation of the capture set of pursuers, as provided in the following theorem.

THEOREM 3. *Pursuer capture set for* $\varepsilon > 0$ *of [2].*
Consider players with dynamics (1) and speed ratio $0 < \sigma < 1$ *(i.e., faster evader). For a pursuer position* x^i *with capture distance* ε, *and evader position* x^e, *the pursuer capture set boundary* $x \in \mathbb{R}^2$ *is given by the Cartesian oval*

$$x = x^e + r(\phi) \begin{bmatrix} \cos(\gamma^i + \phi) \\ \sin(\gamma^i + \phi) \end{bmatrix} \tag{2}$$

where

$$r(\phi) = \frac{\varepsilon\sigma + d^i \cos(\phi) \pm \sqrt{(\sigma\varepsilon + d^i \cos(\phi))^2 - (1 - \sigma^2)(d^{i2} - \varepsilon^2)}}{1 - \sigma^2}$$

for $\phi \in [-\phi^i, \phi^i]$ *given by* $\phi^i = \cos^{-1}\left[\frac{\sqrt{(1-\sigma^2)(d^{i2}-\varepsilon^2)}-\sigma\varepsilon}{d^i}\right]$. *The distance* $d^i = \|x^i - x^e\|_2$, *and* $\gamma^i = \tan^{-1}\left(\frac{x_2^i - x_2^e}{x_1^i - x_1^e}\right)$.

Table 1 Matrix norm $\|A\|_p$ and induced matrix measure $\mu_p(A)$

$\|A\|_p = \max_{\|x\|_p=1} \frac{\|Ax\|_p}{\|x\|_p}$	$\mu_p(A) = \lim_{\delta \to 0^+} \frac{\|I + \delta A\|_p - 1}{\delta}$
$\|A\|_1 = \max_j \sum_{j \neq i} \|q_{ij}\|$	$\mu_1(A) = \max_j \left[q_{jj} + \sum_{j \neq i}^n \|q_{ij}\| \right]$
$\|A\|_2 = \sqrt{\max_i [\lambda_i(A^\top A)]}$	$\mu_2(A) = \max_i \left\{ \lambda_i \left(\frac{A^\top + A}{2} \right) \right\}$
$\|A\|_\infty = \max_i \sum_{i \neq j} \|q_{ij}\|$	$\mu_\infty(A) = \max_i \left[q_{ii} + \sum_{i \neq j}^n \|q_{ij}\| \right]$

2 Multi-Agent Control for Pursuer Coordination in Reach-Avoid Games

This work analyzes a pursuer coordination addressing Problem 1 through multi-agent control. The multi-agent control approach is based on the minimization of the *locational cost,* which treats the pursuers capture sets as resources to be distributed over an environment. The locational cost, which provides the surrogate coverage objective, is defined as follows:

$$\sum_{i=1}^{N} \int_{\mathcal{V}^i(p,t)} \|p^i - q\|^2 dq \tag{3}$$

where $p^i(t) \in \mathcal{M}(t)$ is a mapping of the pursuer's capture-set location to the coverage domain, and $\mathcal{V}^i(p, t)$ constitutes a proper partition of the coverage domain. This partition can account for the size of the individual pursuer's capture set, for instance, $\mathcal{V}^i(p, t) = \{q \in \mathcal{M}(t) | w^i \|q - p^i\| \leq w^j \|q - p^j\|, \forall j \neq i\}$. The work by Refs. [4,7,8] solves the coverage problem in Eq. (3) for the center of the

Apollonius circle with center and radius given by $p^i = [x^i - \sigma^2 x^e]c_\sigma$, $r^i = \|x^i - x^e\|\sigma c_\sigma$, where $c_\sigma = 1/(1-\sigma^2)$. The Apollonius circle fully characterizes a pursuer's capture set provided the particle dynamics in Eq. (1) and a point capture objective, i.e., $\varepsilon = 0$. The pursuer locations were then updated through the relationship

$$\dot{x}^p = (1-\sigma^2)\dot{p} + \sigma^2 \dot{x}^e \tag{4}$$

A gradient descent controller for minimizing (3) is provided by Lloyd's algorithm shown by [5]:

$$\dot{p} = \kappa(c(p,t) - p) \tag{5}$$

where $c(p,t)$ is the time-varying vector of center of mass for each partition $\mathcal{V}^i(p,t)$. A Lyapunov-based controller for minimizing (3) is provided by the time-varying domain (TVD) controller developed by [6]:

$$\dot{p} = \left(I - \frac{\partial c(p,t)}{\partial p}\right)^{-1}\left(\kappa(c(p,t)-p) + \frac{\partial c(p,t)}{\partial t}\right) \tag{6}$$

for some gain $\kappa > 0$.

Further consider $\mathcal{M}(t)$ is represented by a nonintersecting curve $\gamma : [0, L] \times \mathbb{R}_{\geq 0} \to \mathcal{M}(t)$, where L is the time-varying arc-length of $\mathcal{M}(t)$. Then, defining the time-varying domain reference locations $\hat{r}_1(t) := 0$ and $\hat{r}_2(t) := L$ allows us to obtain the desired time-varying centers of mass $c(p,t)$ as a function of agent weights w^i as provided by Ref. [3]. The next section provides the different problems addressed in this work.

3 Problem Description

It was shown by [3] that $c(p,t) = \frac{\partial c}{\partial p}p + B\hat{r}(t)$. Defining $L_f \triangleq I - \frac{\partial c}{\partial p}$, the dynamics in Eqs. (5) and (6) reduce to

$$\dot{p} = -\kappa L_f p + \kappa B\hat{r}(t) \quad \text{(Lloyd's)} \tag{7}$$

$$\dot{p} = -\kappa p + \kappa L_f^{-1} B\hat{r}(t) \quad \text{(TVD)} \tag{8}$$

where the feed forward term $\partial c(p,t)/\partial t$ is set to zero for comparison purposes. Then, the difference between Lloyd's and the TVD tracking dynamics arises from the partition scheme used to calculate the center of mass $c(p,t)$. Under the multiplicatively weighted partition, information from all pursuers is needed to perform the matrix inverse L_f^{-1}, whereas only nearest-neighbor information is needed to compute L_f. Thus, TVD would provide a centralized controller topology, while Lloyd's provides a distributed controller topology. Under uniform domain partitions, both formulations are distributed.

The desired pursuer capture-set configuration in both Eqs. (7) and (8) is given by $\bar{p} \triangleq L_f^{-1}B\hat{r}(t)$. This desired configuration encapsulates the surrogate coverage objective; thus, exactly satisfying it leads to guaranteed capture. However, this configuration cannot be exactly achieved because of the controller's finite response time. Furthermore, once the desired capture-set dynamics are obtained, they are mapped through (4) and further subject to saturation. Thus, the objective of this work is to provide a quantitative method of accounting for the controller's finite response time and pursuer saturation constraints when the pursuers track the desired capture-set configuration.

First, the tracking performance of Lloyd's and the TVD controllers at the capture-set level is analyzed. Second, the saturation effect at the pursuer level is analyzed as follows. Assume that there exists an invertible function $\hat{p} = h(\hat{x}^p, x^e(t))$, such that $\hat{x}^p = h^{-1}(\hat{p}, x^e(t))$, and define the desired pursuer configuration $\bar{x}(t)$ by $p = h(\bar{x}, x^e(t))$. To make the analysis tractable, we reformulate the pursuer configuration dynamics using the smooth saturation function

$$\dot{x}^p = \bar{u}^p \,\mathrm{sat}(\kappa(\bar{x}(t) - x^p)) \tag{9}$$

The saturation function is applied component-wise, i.e., for $y \in \mathbb{R}^n$,

$$\mathrm{sat}(y) = \left[\frac{2}{1+e^{-2y_1}} - 1, \ \ldots, \ \frac{2}{1+e^{-2y_n}} - 1\right]^\top \tag{10}$$

Finally, the worst-case tracking error for system (9) given by $\|\bar{x}(t) - x^p(t)\|_\infty$ will be related to the sufficient number of pursuers needed to provide capture guarantees.

4 Relating Tracking Performance to Capture Guarantees

In this section, contraction theory is first used to characterize the impact of the coverage controller topology in tracking performance. Then, an upper bound will be obtained for the error dynamics system (9) that characterizes how the pursuers with maximum speed saturation can track the desired pursuer capture-set configuration. A circular description for the pursuer capture set will then be provided. Finally, the results are combined to provide a verification condition for the sufficient number of pursuers.

4.1 Tracking Performance at the Capture-Set Level.

The matrices composing the desired capture-set center dynamics, as originally derived by Ref. [7], are now provided.

Definition 1 (Weighted Laplacian). *The adjacency matrix for the pursuers is given by* $A \in \mathbb{R}^{N\times N}$, *where* $[A]_{ij} = \frac{1}{2}\frac{w^j}{w^i + w^j}$ *if* $j = i+1$ *or* $j = i-1$ *and* $[A]_{ij} = 0$ *otherwise. Hence, A is tridiagonal. Further, the pursuer i's neighborhood set by* $\mathcal{N}^i = \{j \in [N] \mid [A]_{ij} \neq 0\}$. *The in-degree matrix is given by* $D_{in} \in \mathbb{R}^{N\times N}$ *with* $D_{in} = \mathrm{diag}(A1_N)$. *This results in the Laplacian matrix* $L = D_{in} - A$. *Further defining* $B_r = \mathrm{diag}(1, 0_{1\times N-2}, 1) \in \mathbb{R}^{N\times N}$ *leads to the grounded Laplacian matrix* $L_f(\alpha) = L(\alpha) + \frac{1}{2}B_r$, *where* $\alpha_{ij} = \frac{w^j}{w^i + w^j}$.

Remark 1. Given the leader-follower structure of $L_f(\alpha)$, it is invertible as shown by Ref. [7].

Definition 2 (Actuation Matrix). *Given N pursuers, the actuation matrix is given by* $B = \frac{1}{2}\begin{bmatrix} 1 & 0_{N-2} & 0 \\ 0 & 0_{N-2} & 1 \end{bmatrix}^\top \in \mathbb{R}^{N\times 2}$.

Note that the dynamics can be extended to $p^i \in \mathbb{R}^2$ through the Kronecker product

$$\dot{p} = \kappa\big((- L_f(\alpha) \otimes I_2)p + (B \otimes I_2)\hat{r}(t)\big)$$

Based on these definitions, the following useful Lemmas are now provided.

Lemma 1. $-L_f 1 = -\frac{1}{2}B_r 1_N$.

Proof. Based on Definition 1, $A \geq 0$ (component-wise), $\mathrm{diag}(A) = 0$ and $D_{\text{out}} = \mathrm{diag}(A1)$. Because $(A - D_{\text{out}})1 = 0$, it follows that $-L_f 1 = -\frac{1}{2}B_r 1$. ∎

Lemma 2. *For* $N = 2$, $\mu_\infty(L_f(\alpha)) = -1/2$. *For* $N \geq 3$, $\mu_\infty(L_f(\alpha)) = 0$ *for any* α.

Proof. Follows by Definition 1 and Lemma 1. Given $-L_f = A - D_{\text{out}} - \frac{1}{2}B_r$, where B_r is also diagonal, it follows that $\mu_\infty(-L_f) = \max(-L_f 1)$. ∎

Lemma 3. *For a fixed set of parameters* α, $0 < \mu_2(L_f(\alpha)) \leq \frac{1}{2}$.

Proof. Note that the matrix $L_s = \frac{1}{2}(L_f(\alpha)^\top + L_f(\alpha))$ can be written as $L_s(\alpha) = L_u(\alpha) + \frac{1}{2}B_r$, where $L_u(\alpha) = \frac{1}{2}(L(\alpha) + L(\alpha)^\top) = L(\alpha)^\top$. From (Theorem 1 of [12]), it follows that $0 < \lambda_1(L_s) \leq \frac{1}{2}$. ∎

Table 2 Contraction rate summary

	$\mu_\infty(A)$		$\mu_2(A)$	
	$N=2$	$N\geq 3$	$N=2$	$N\geq 3$
$A=-\kappa L_f(\alpha)$	$-\frac{1}{2}\kappa$	0	$-\frac{1}{2}\kappa$	$[-\frac{1}{2}\kappa, 0)$
$A=-\kappa I$	$-\kappa$	$-\kappa$	$-\kappa$	$-\kappa$

Defining the error $z=p-L_f(\alpha)^{-1}B\hat{r}(t)$, the error dynamics for the systems in Eqs. (7) and (8) are given by

$$\dot{z}_L=-\kappa L_f(\alpha)z_L-L_f^{-1}(\alpha)B\dot{\hat{r}}(t), \quad \text{(Lloyd's error)} \tag{11}$$

$$\dot{z}_T=-\kappa z_T-L_f^{-1}(\alpha)B\dot{\hat{r}}(t) \quad \text{(TVD error)} \tag{12}$$

THEOREM 4. *The TVD controller has a better tracking performance bound than Lloyd's in the $\infty-$ norm for $N=2$, and in the 2-norm for $N\geq 2$.*

Proof. The contraction rates for (11) and (12), which build on Lemmas 2 and 3, are summarized in Table 2. Thus, both systems are contracting by Theorem 1. Notice how both error dynamics in (11) and (12) are subject to the same disturbance $L_f^{-1}(\alpha)B\dot{\hat{r}}(t)$. Further assuming the disturbances are bounded, from Theorem 2, one can easily see that any difference in tracking performance upper bound will arise from differences in the contraction rate. Thus, the claim follows. ∎

Remark 2. Although the primary interest is on $\|p-\bar{p}\|_\infty$, the Laplacian structure of the follower agents in L_f prevents us from obtaining a contraction rate for $\mu_\infty(-L_f)$ when $N>2$. Thus, given $\|p-\bar{p}\|_\infty\leq\|p-\bar{p}\|_2$, results for the 2-norm are provided.

Several design considerations can be concluded from Theorem 4.

(1) The TVD tracking controller in Eq. (8) produces better tracking performance bounds than Lloyd's (7).
(2) If a centralized implementation of Eq. (8) is not feasible, then a consensus filter or observer with a contraction rate larger than $1/2\kappa$ would provide better performance than (7).
(3) A distributed version of Eq. (8) can also be realized through a Neumann series expansion (shown by Ref. [13]) of the term $L_f(\alpha)^{-1}=(I+\frac{\partial c}{\partial p})^{-1}\approx\sum_{i=0}^{m}\left(\frac{\partial c}{\partial p}\right)^i$, where m is the available number of hops as demonstrated by Ref. [5]. However, note that for a suitable $p-$ norm, the Neumann series has a truncation error $s_p=\frac{\|\partial c/\partial p\|_p^{m+1}}{1-\|\partial c/\partial p\|_p}$. Thus, an advantage over the formulation in Eq. (7) can be proven if $s_2+\frac{\|L_f(\alpha)^{-1}B\dot{\hat{r}}(t)\|_2}{\kappa}<2\frac{\|L_f(\alpha)^{-1}B\dot{\hat{r}}(t)\|_2}{\kappa}$.

4.2 Tracking Performance at the Pursuer Level. At this stage, it is assumed that a tracking controller at the capture-set level has been selected, and the attention is shifted to the tracking of this reference signal by the pursuers with saturated dynamics (9). First, consider an autonomous system under saturation

$$\dot{y}=\text{sat}(-\kappa y) \tag{13}$$

where $y\in\mathbb{R}^n$ and $\kappa>0$.

LEMMA 4. *For an initial condition $y(0)=y_0$, system (13) evolves in a bounded domain $\mathcal{Y}=\{y\in\mathbb{R}|y^\top y\leq y_0^\top y_0\}$.*

Proof. Define a Lyapunov function $V=\frac{1}{2}y^\top y$. Note that its derivative $\dot{V}=y^\top\text{sat}(-\kappa y)<0$ for all $y\setminus\{0\}$, which makes (13) Lyapunov stable. The claim follows given the negative definiteness of the Lyapunov function derivative. ∎

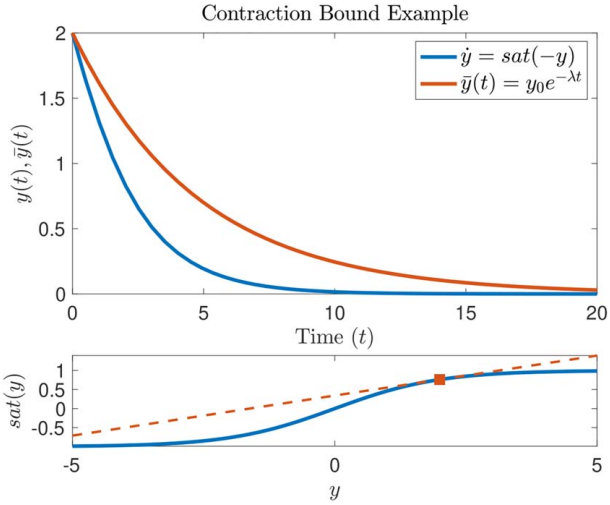

Fig. 1 Top panel: For system $\dot{y}=\text{sat}(-y)$ with initial conditions $y(0)=2$, the system trajectory is given by the blue line, and the contraction upper bound is given by the orange line. Bottom panel: The contraction rate is provided by the slope of the saturation function evaluated at the set boundary, which is $y=2$.

LEMMA 5. *System (13) is contracting under any metric.*

Proof. First note that the Jacobian is diagonal with entries $\frac{d\text{sat}(-\kappa y_i)}{dy_i}$. From Eq. (10), note that $\frac{d\text{sat}(-\kappa x)}{dx}\in[-\kappa, 0)$ for $\kappa>0$. Because $y(t)$ evolves in a bounded set by Lemma 4, it follows that $\exists\lambda$ such that $\frac{d\text{sat}(-\kappa y_i)}{dy_i}\leq-\lambda\ \forall i$. Thus, the system is contracting with contraction rate λ in any metric given the diagonal structure of the dynamics. ∎

A pictorial representation of Lemma 5 is provided in Fig. 1.

The error dynamics for system (9) are given by

$$\begin{aligned}\bar{z}&=x^p-\bar{x}\\ \dot{\bar{z}}&=\text{sat}(-\kappa\bar{z})-\dot{\bar{x}}\end{aligned} \tag{14}$$

THEOREM 5. *For a bounded $\|\dot{\bar{x}}\|_\infty\leq d$, the tracking error is bounded by*

$$\|x^p(t)-\bar{x}(t)\|_\infty\leq\chi_0e^{-\lambda t}+\frac{d}{\lambda} \tag{15}$$

where λ is the contraction rate of the autonomous system $\dot{z}=\text{sat}(-\kappa z)$.

Proof. Note that system $\dot{\bar{z}}=\text{sat}(-\kappa\bar{z})-\dot{\bar{x}}$ is a perturbed version of system $\dot{z}=\text{sat}(-\kappa z)$, which is contracting by Lemma 5. Now, the error $\|z-\bar{z}\|_\infty\leq\|z\|_\infty+\|\bar{z}\|_\infty$ by the triangular inequality. The rest follows by applying Theorem 1 to upper bound $\|z\|_\infty$ and Theorem 2 to upper bound $\|\bar{z}\|_\infty$. ∎

Remark 3. Lemma 5 and Theorem 5 are intended to formalize the approach followed in practice where input saturation is dealt with by decreasing the feedback gain.

4.3 Minimum Number of Pursuers Condition. For an RA game in finite time, Ref. [8] shows that there exists a critical coverage domain length the pursuers' capture sets need to span to provide capture guarantees. This coverage domain $\mathcal{M}(t)$ is given by a line segment, and as Ref. [8] demonstrates, the capture-set overlap must be analyzed for the minimum spanning pursuer configuration, which has the evader located at the center. Thus, we now focus on combining the tracking dynamics error in Theorem 5 with the pursuer capture set in Eq. (2) to provide a verifiable overlap condition for the minimum spanning pursuer configuration.

4.3.1 Capture Set for Minimum Spanning Pursuer Configuration. The proposed expression for the boundary of the capture set is given by

$$\begin{aligned} r^i &= \tfrac{\varepsilon}{1-\sigma^2} + \tfrac{\sigma}{1-\sigma^2} d^i \\ o^i &= \left(\tfrac{\varepsilon\sigma}{1-\sigma^2} + \tfrac{1}{1-\sigma^2} d^i\right) \begin{bmatrix} \cos(\gamma^i) \\ \sin(\gamma^i) \end{bmatrix} \end{aligned} \tag{16}$$

where o^i is the center and r^i is the radius.

PROPOSITION 1. *The capture with boundary in Eq. (16) exactly matches the Cartesian oval (2) for the minimum spanning pursuer configuration.*

Proof. First, the minimum spanning pursuer configuration has the evader located at the origin of the coverage domain $x^e = (0, 0)$ and the pursuers' centers contained in a line segment. Thus, let us consider the orientation $\phi = 0$ in expression (2). This provides two boundary points $r(0) = \dfrac{\varepsilon\sigma + d^i \pm (\varepsilon + \sigma d^i)}{1-\sigma^2}$. The diameter for a circle whose chord contains these two points has a length $D^i = \dfrac{2\varepsilon + 2\sigma d^i}{1-\sigma^2}$. Thus, the radius expression follows. The center follows by adding $r^i[\cos(\gamma^i)\ \sin(\gamma^i)]^\top$ to the point $\dfrac{\varepsilon\sigma + d^i - (\varepsilon + \sigma d^i)}{1-\sigma^2}[\cos(\gamma^i)\ \sin(\gamma^i)]^\top$, which corresponds to the negative sign term for $r(0)$. ∎

4.3.2 Static and Dynamic Conditions for Capture. Let us recall Theorem 5, and define a time $\bar{t}$ such that $\chi_0 e^{-\lambda\bar{t}} \triangleq (\beta - 1)\dfrac{d}{\lambda}$ for $\beta > 1$. Then for $t \geq \bar{t}$, it follows that

$$\|x^p - \bar{x}\|_\infty \leq \beta \frac{d}{\lambda} \tag{17}$$

Now, given an $\varepsilon-$ Capture distance, a sufficient number of pursuers will be selected such that if the distance between two pursuers is maximized given (17), the pursuers' capture set in Eq. (16) still overlaps along the direction $\gamma^i = 0$ without loss of generality.

In what follows, an ordering of the pursuers is assumed such that $o^{i+1} > o^i$ on the coverage domain $\mathcal{M}(t)$. The minimum capture-set overlapping condition is provided by

$$\begin{aligned} g &= o^{i+1} - r^{i+1} - (o^i + r^i) \\ (1-\sigma^2)g &= d^{i+1} - d^i + \delta d^{i+1} - \delta d^i \\ &\quad - 2\varepsilon - \sigma|d^{i+1} + \delta d^{i+1}| - \sigma|d^i + \delta d^i| \end{aligned} \tag{18}$$

where g is the gap between consecutive circles and δd^i is the dynamic tracking error for the ith circle. Note that $-\beta\frac{d}{\lambda} \leq \delta d^j \leq \beta\frac{d}{\lambda}$, for $j \in \{i, i+1\}$. The next theorem provides a verification condition to ensure the capture sets overlap.

THEOREM 6. *For the cost definition in (18), the problem*

$$\begin{aligned} &\operatorname{argmax}_{\delta d^i,\, \delta d^{i+1}}\ g(\delta d^i, \delta d^{i+1}) \\ &\text{s.t. } -\beta\frac{d}{\lambda} \leq \delta d^j \leq \beta\frac{d}{\lambda} \ \text{for} j \in \{i, i+1\} \end{aligned} \tag{19}$$

has solution $\delta d^i = -\beta\dfrac{d}{\lambda}$, $\delta d^{i+1} = \beta\dfrac{d}{\lambda}$.

Proof. Note that the gradient of the cost is given by

$$\nabla J = \begin{bmatrix} -1 - (-1)^m\sigma \\ 1 - (-1)^n\sigma \end{bmatrix}$$

where the values (m, n) are determined by the sign condition of the absolute value. This gradient cannot equal zero for any value inside the domain given $0 < \sigma < 1$. Thus, the maximum value is reached at the boundary of the convex domain. A simple search over the boundary yields the result. ∎

Based on Theorem 6, the pursuer's capture sets are at least tangential if

$$\underbrace{d^{i+1} - d^i}_{\text{Static}} + \underbrace{2\bar{\delta} - \sigma|d^{i+1} + \bar{\delta}| - \sigma|d^i - \bar{\delta}|}_{\text{Dynamic}} - \underbrace{2\varepsilon}_{\text{Radius}} \leq 0 \tag{20}$$

for $\bar{\delta} = \beta\dfrac{d}{\lambda}$. The terms labeled static correspond to the desired location for the minimum spanning pursuer configuration. The terms labeled dynamic arise from the worst-case tracking performance of the pursuers subject to saturation. The nonzero capture radius is given by -2ε. Note that increasing the speed ratio σ and the

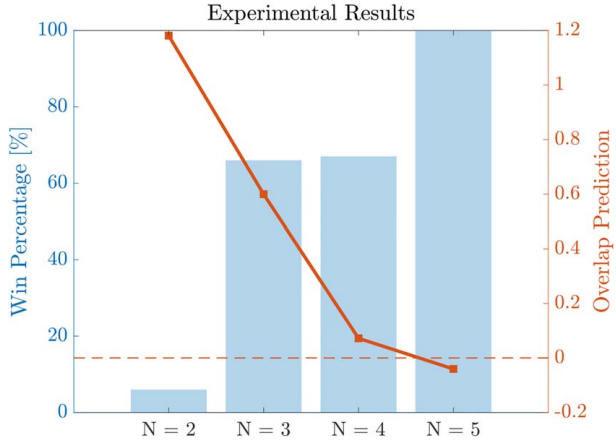

Fig. 2 Numerical results summary. The coverage-based pursuer strategy required $N = 5$ to successfully capture the evader in all considered scenarios. The blue bars show the percentage of scenarios where pursuer capture was achieved. The orange curve depicts the worst-case pursuer capture-set overlap prediction from expression (20). Thus, the pursuer team size prediction corresponds to the first instance for which this value falls below zero. This is provided by $N = 5$.

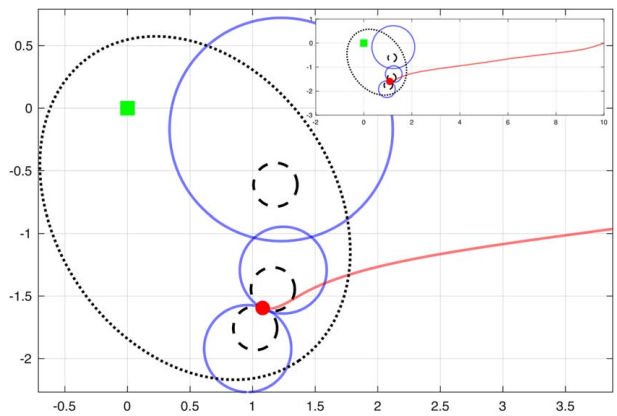

Fig. 3 Example scenario for $N = 3$. All simulations were performed for $\sigma = 0.5$, $\varepsilon = 0.175$, $\bar{v}_e = 1$, and $t_f = 15$. The defended area is given by the green box at (0, 0). The blue circle corresponds to the capture set approximation in (16), whose center is the desired quantity to be controlled, and the black dashed circle shows the capture distance for each individual pursuer. The red curve corresponds to the evader trajectory, and the dotted ellipse corresponds to the evader's constrained reachable set. Note how the evader tries to maneuver between the bottom two pursuers, but ultimately enters the capture region.

capture radius ε, or decreasing the tracking error $\bar{\delta}$, makes the inequality easier to verify, as is to be expected.

5 Simulation Results

A simulation testbed was developed in MATLAB R2021b for an RA game against a fast evader with finite time t_f. Similar to the work of Ref. [8], a prescribed coverage domain distance is provided, thus defining the $\hat{r}(t)$ values as the intersection of a line orthogonal to the $y-$ axis and the evader's constrained reachable set. To prevent capture, the evader executes the optimal strategy outlined in Theorem 4 of Ref. [2], which seeks to maximize the gap between two consecutive pursuers. The simulation results randomize both the initial location of the pursuers and the two consecutive pursuers selected for the evader to breach. One hundred Monte Carlo simulations were performed for a team of $N = \{2, \ldots, 5\}$ pursuers.

For a given pursuer gain κ, the saturation level $\bar{s}$ was recorded in simulation for all scenarios. Then the tracking bound was estimated by solving for the upper bound $\text{sat}\left(\kappa\beta\frac{d}{\lambda}\right) = \bar{s}$ and selecting the maximum value for $\beta\frac{d}{\lambda}$ across all scenarios. The simulation results are summarized in Fig. 2. The blue bars quantify the win percentage for a pursuer team size N. Note that large percentage increase occurs when an odd number of pursuers is selected. This is due to the evader policy developed by Ref. [2] successfully creating gaps between the two central pursuers when N is even.

The orange line is the evaluation of Eq. (20). The minimum number of pursuers predicted by (20) is $N = 5$, which corresponds to the smallest N for which the expression becomes negative. Note that this is in accordance with the simulated win percentage. An example run, along with the simulation parameters, is provided in Fig. 3.

6 Conclusions

This work presents the application of control theoretical tools for developing a verifiable condition for capture guarantees in cooperative pursuer strategies. The analyzed cooperative pursuer strategy is based on coverage control whose objective is to separate the evader from its goal in finite-time RA games. A minimum overlap requirement for the pursuers' capture set in a critical configuration was developed, and its predictive capability was highlighted in simulation. The developed approach combines tools from differential games and contraction theory to combine the geometric and dynamic requirements for a team of N pursuers to capture a faster evader.

Conflict of Interest

There are no conflicts of interest.

Data Availability Statement

The datasets generated and supporting the findings of this article are obtainable from the corresponding author upon reasonable request.

References

[1] Weintraub, I. E., Pachter, M., and Garcia, E., 2020, "An Introduction to Pursuit-Evasion Differential Games," 2020 American Control Conference (ACC), Denver, CO, July 1–3, IEEE, pp. 1049–1066.

[2] Garcia, E., and Bopardikar, S. D., 2021, "Cooperative Containment of a High-Speed Evader," 2021 American Control Conference (ACC), New Orleans, LA, May 25–28, IEEE, pp. 4698–4703.

[3] Rivera-Ortiz, P., and Diaz-Mercado, Y., 2018, "On Guaranteed Capture in Multi-player Reach-Avoid Games via Coverage Control," IEEE Control Syst. Lett., **2**(4), pp. 767–772.

[4] Rivera-Ortiz, P., Diaz-Mercado, Y., and Kobilarov, M., 2020, "Multi-Player Pursuer Coordination for Nonlinear Reach-Avoid Games in Arbitrary Dimensions via Coverage Control," 2020 American Control Conference (ACC), Denver, CO, July 1–3, IEEE, pp. 2747–2753.

[5] Lee, S. G., Diaz-Mercado, Y., and Egerstedt, M., 2015, "Multirobot Control Using Time-Varying Density Functions," IEEE Trans. Robot., **31**(2), pp. 489–493.

[6] Xu, X., and Diaz-Mercado, Y., 2020, "Multi-agent Control Using Coverage Over Time-Varying Domains," 2020 American Control Conference (ACC), Denver, CO, July 1–3, IEEE, pp. 2030–2035.

[7] Davydov, A., Rivera-Ortiz, P., and Diaz-Mercado, Y., 2021, "Pursuer Coordination in Multi-Player Reach-Avoid Games Through Control Barrier Functions," 2021 American Control Conference (ACC), New Orleans, LA, May 25–28, IEEE, pp. 3222–3227.

[8] Khrenov, M., Rivera-Ortiz, P., and Diaz-Mercado, Y., 2021, "On the Geometric Feasibility of Defense Manifold Maintenance in Planar Reach-Avoid Games Against a Fast Evader," 2021 Modeling, Estimation and Control Conference (MECC), Austin, TX, Oct. 24–27, IFAC.

[9] Lohmiller, W., and Slotine, J.-J. E., 1998, "On Contraction Analysis for Non-linear Systems," Automatica, **34**(6), pp. 683–696.

[10] Del Vecchio, D., and Slotine, J.-J. E., 2012, "A Contraction Theory Approach to Singularly Perturbed Systems," IEEE Trans. Automat. Contr., **58**(3), pp. 752–757.

[11] Isaacs, R., 1999, *Differential Games: A Mathematical Theory with Applications to Warfare and Pursuit, Control and Optimization*, Courier Corporation, North Chelmsford, MA.

[12] Xia, W., and Cao, M., 2017, "Analysis and Applications of Spectral Properties of Grounded Laplacian Matrices for Directed Networks," Automatica, **80**, pp. 10–16.

[13] Stewart, G. W., 1998, *Matrix Algorithms Volume 1: Basic Decompositions*, SIAM, Philidelphia, PA.